Presentation of admission to the Final Exam

Tethers for Deorbit of Objects in High Eccentricity Orbits at the End-of-Life

PhD Student *Ing. Guido PASTORE*

Supervisor *Prof. Enrico LORENZINI*
Co-Supervisor *Ing. Marco PERTILE*

PhD Course in *Scienze, tecnologie e misure spaziali*
Curricolo *Misure Meccaniche per l'ingegneria e lo spazio*
XXX Cycle

INTRODUCTION

Deorbit target: Sylda

25-year deorbit on future objects launched to space would lead in 100 years to **< 10 catastrophic collisions** instead than **more than 50 with business-as-usual scenario** (Klinkrad H., 2006)

294 mission-related objects left in **GTO** between 2004 and 2012**: only 43 reentered** (Fisher, S. and David, E., 2014)

Dual-payload adapters are a **threat to operational satellites: mass** of about **500 kg** and **very large exposed area.**

Example: *Sylda,* used in *Ariane5,* left in GTO.

Deorbit from GTO has **commercial relevance**

Only in 2014:
5 launches with Ariane5,
all of them to GEO (Ref. . http://www.spacelaunchreport.com/log2015.html)

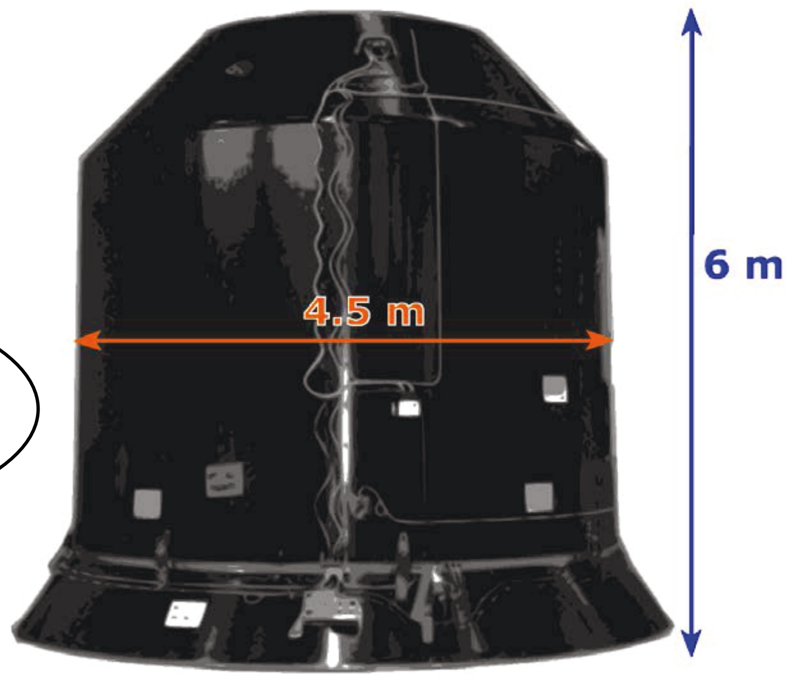

© *Courtesy of ESA*

Main solutions attempted:

- **lower perigee, 200 kg less** onboard **Ariane 5**
- **launch in favorable Sun-synchronous resonance conditions:** no warranty of deorbit time lower than 25 years

Orbital Debris problem

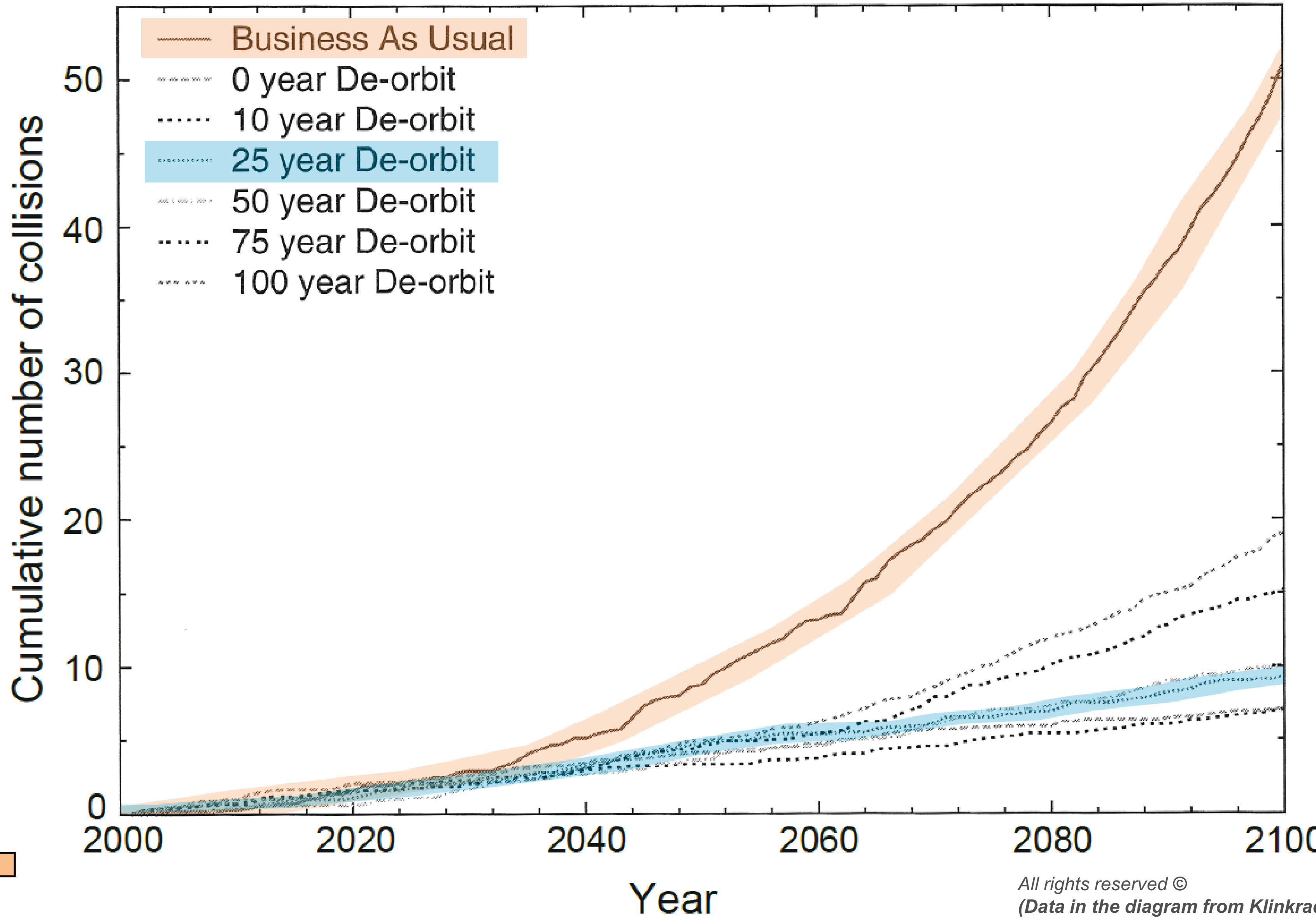

(Data in the diagram from Klinkrad)

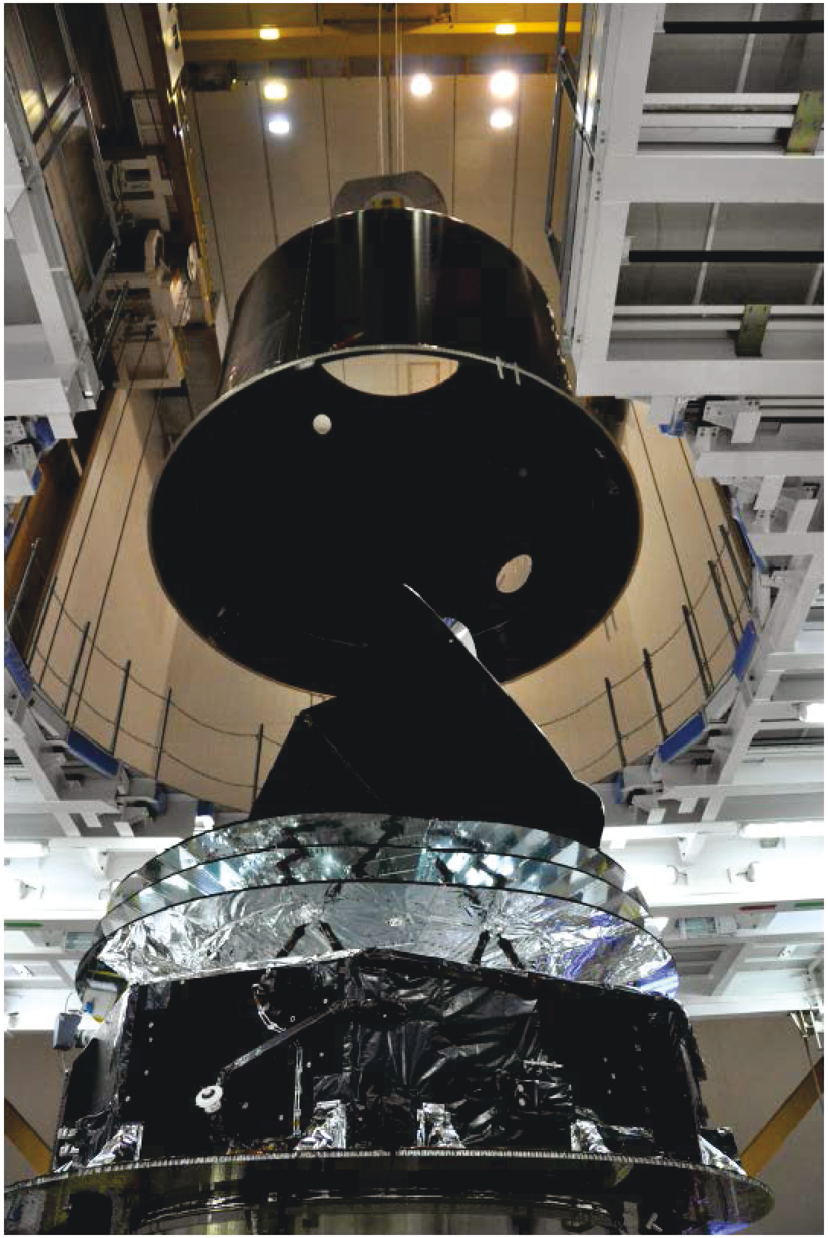

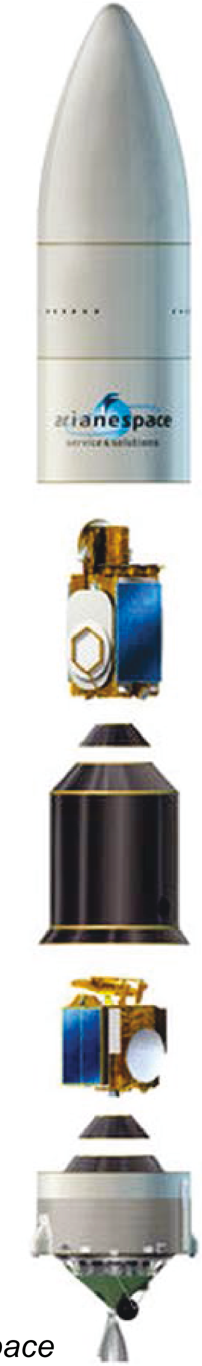

© Courtesy of ESA and Ariane Space

← *Ariane 5* dual-payload and *Sylda*

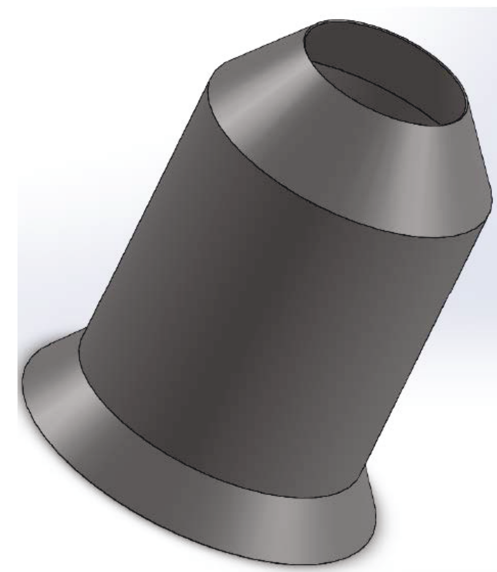

A model in Solidworks was created to determine features not available directly in literature such as moments of inertia.

$$J_x = J_y = 3459\, kg\ m^2$$

$$J_z = 2632\, kg\ m^2$$

Why deorbit from High-Eccentricity Orbits (HEO)?

Predictable applicability to all dual-payload launches to GEO, released in GTO, and to other targets in HEOs, such as inactive satellites in Molnija orbits.

Very little is present in literature.

Possibility of exploiting local rotation for tether attitude stability.

Deorbit is performed dissipating orbital energy and consequently decreasing the orbital altitude

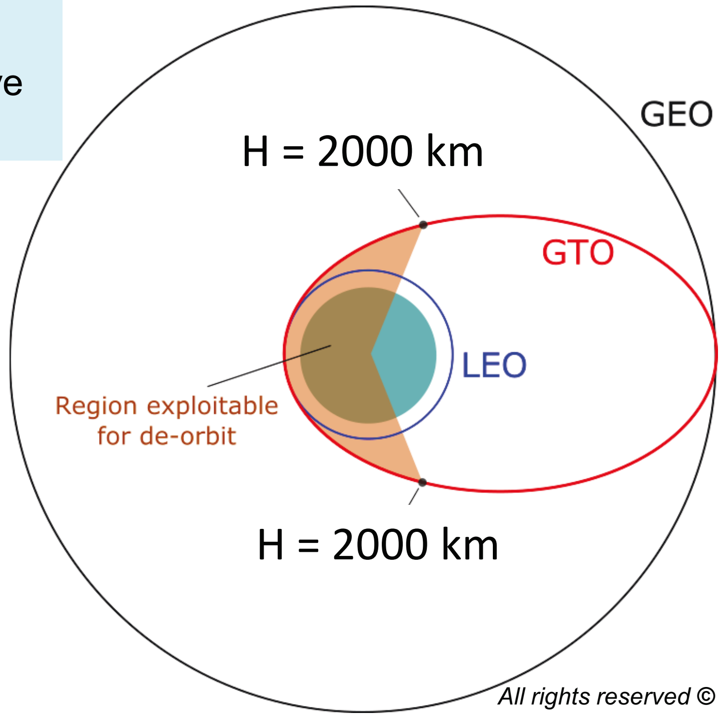

Electrodynamic, or Lorentz, drag: generated by the Bare Electrodynamic Tether

Atmospheric drag: augmented by the Bare Electrodynamic Tether due to its high exposed area.

Energy dissipation computed in the codes only when the system is orbiting below 2000 km for electrodynamic drag, and below 900 km for aerodynamic drag too.
Need sufficient electron density and atmospheric density.

Generation of Lorentz drag with the BET

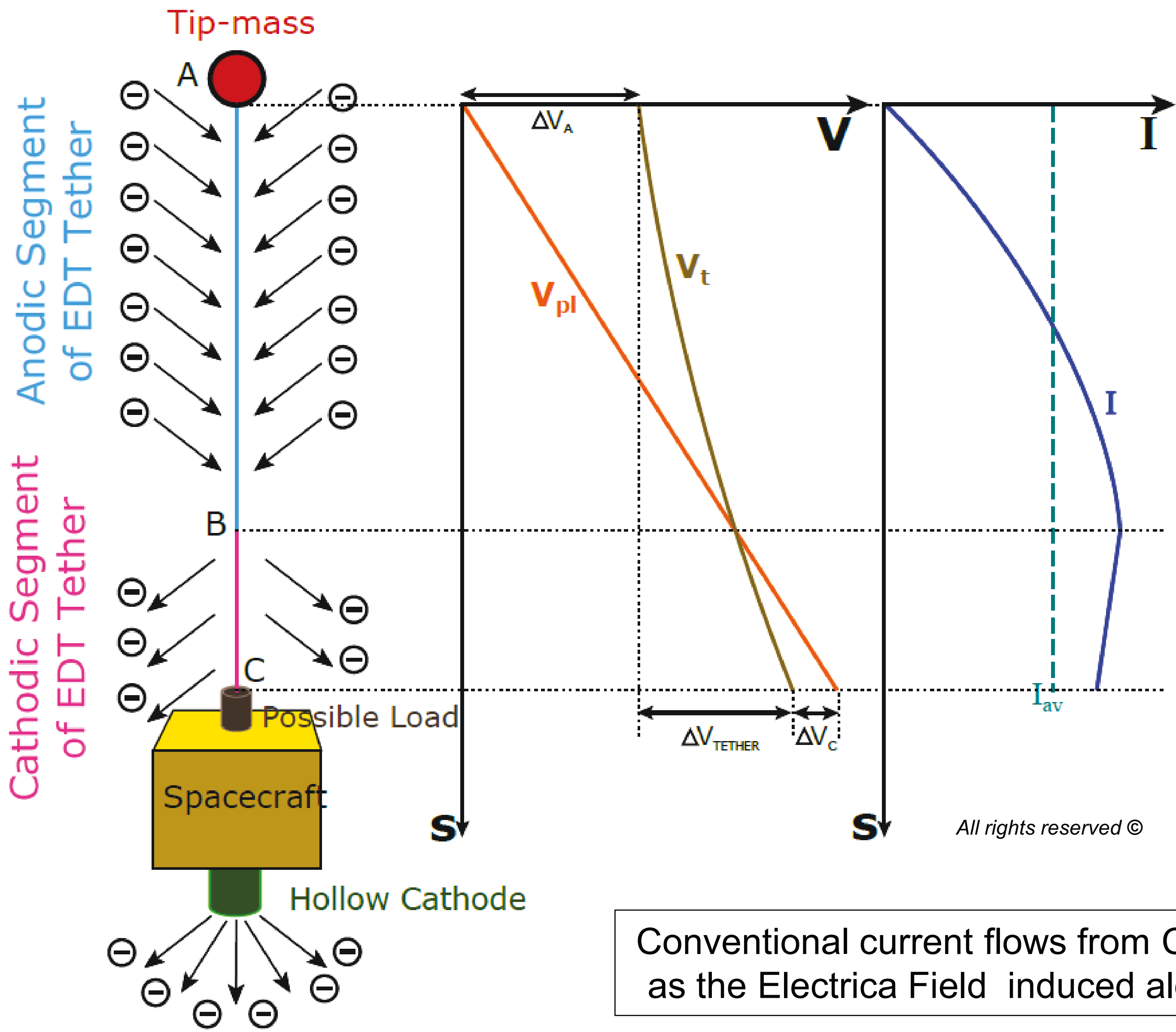

Conventional current flows from C to A, directed as the Electrica Field induced along the tether

Global and local motion of BET system in HEO

***Global motion*: deorbit path of the system's center of mass**
Change in orbital parameters at every computational step during deorbit. Orbital energy dissipation is active only when altitude is below 2000 km.

***Local motion*: rotation of the system around its center of mass.**
Prominent rotation on the orbital plane, but also out-of-plane oscillations are present. In-plane rotation exploited for tether's attitude stabilization.

Part 1

ANALYSIS of DEORBIT

Dumbbell with **Bare Electrodynamic tape Tether**, and **point masses** at anodic tip A and cathodic tip C, (where the cathode and Sylda are placed)

Only in-plane rotation is considered + zero orbital inclination

Normalized parameters and equations are used for higher computational efficiency, following the notation by *Peláez et al.*

$\Lambda_t = m_t / m$ ratio between tether mass and total mass

$X_G = L_t \cos^2 \phi$ distance between C and center of mass G

$h_t = 100 \mu m$

$L_t = 2 km$

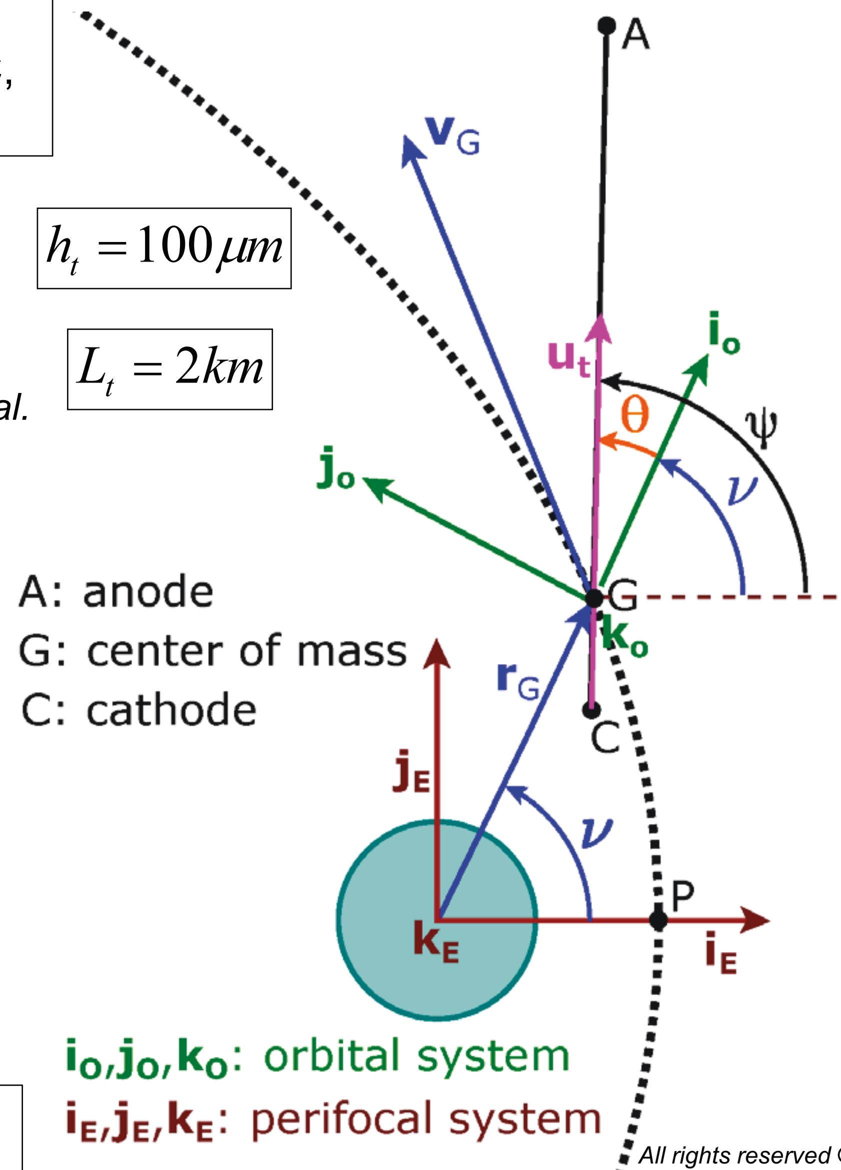

Dipole model is used for the **geomagnetic field**

IRI database from NASA is used for **plasma electron density**, with **average Solar flux**. Variation only with altitude.

Jacchia-Bowman 2008, with **average Solar flux**, is used for **air density**

Aluminum 1100 is used as **conductive tether material.**
Model is valid also with other materials.
If using composite Fiber-Reinforced Aluminum load margins are larger.

Refer to PhD thesis after its publication.

Equations of system's dynamics
(Gauss eqs. from *Bate*, local rotation equation from *Beletsky*)

Orbital Motion Limited current collection and ***Ideal* Tether** (zero cathodic impedance and voltage drop)

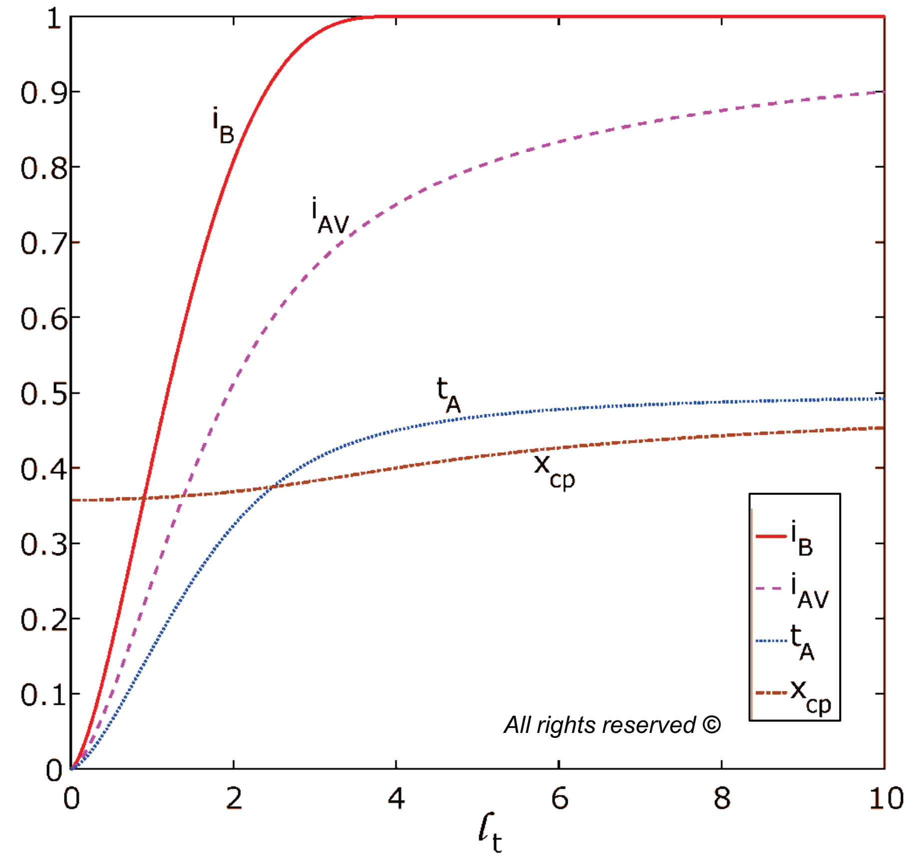

Normalized perturbative force: Lorentz drag and atmospheric drag

Refer to PhD thesis after its publication.

Normalized Lorentz torque about center of mass G

Tension at center of mass, divided by allowed tension from tether's material, including safety factor

1° Analysis campaign – Single case analysis

Full deorbit simulation for a single system's configuration: $\phi = 0.99\phi_0$

ϕ Controls the mass distribution along the system. *Self-balanced* system: a tethered system with where $\phi = \phi_0$ is the value that makes the Lorentz torque to vanish at initial perigee.

Eccentricity and apogee radius: constantly decreasing trend. Steep decrease in the last part, due to higher time spent at altitudes lower than 2000 km where perturbation drag forces are present.

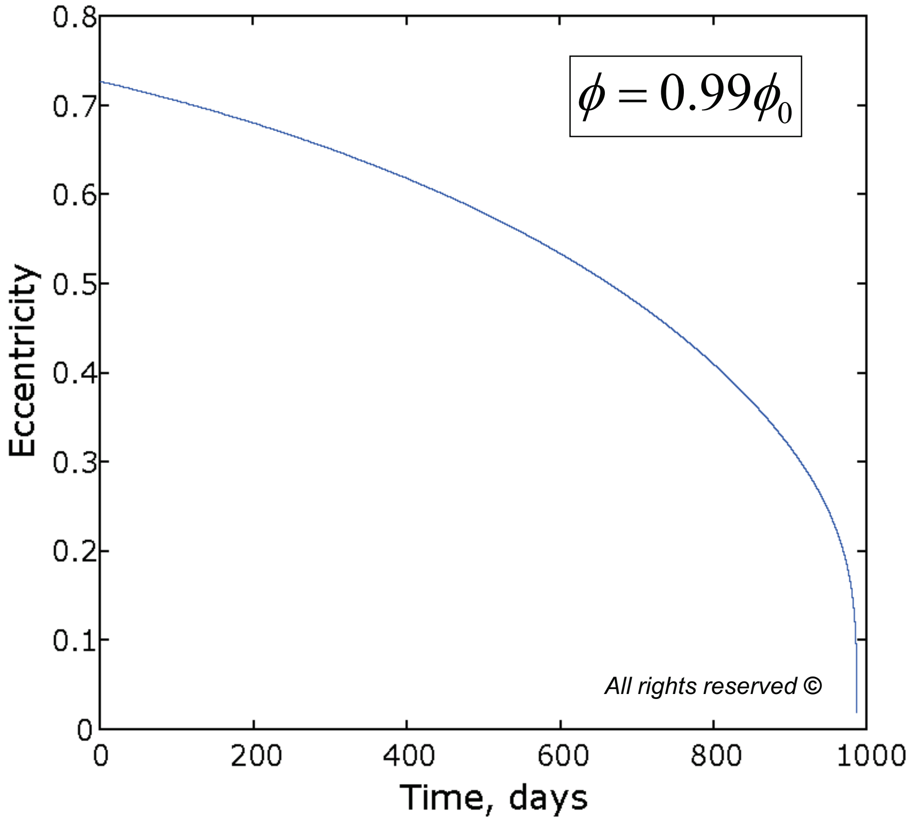

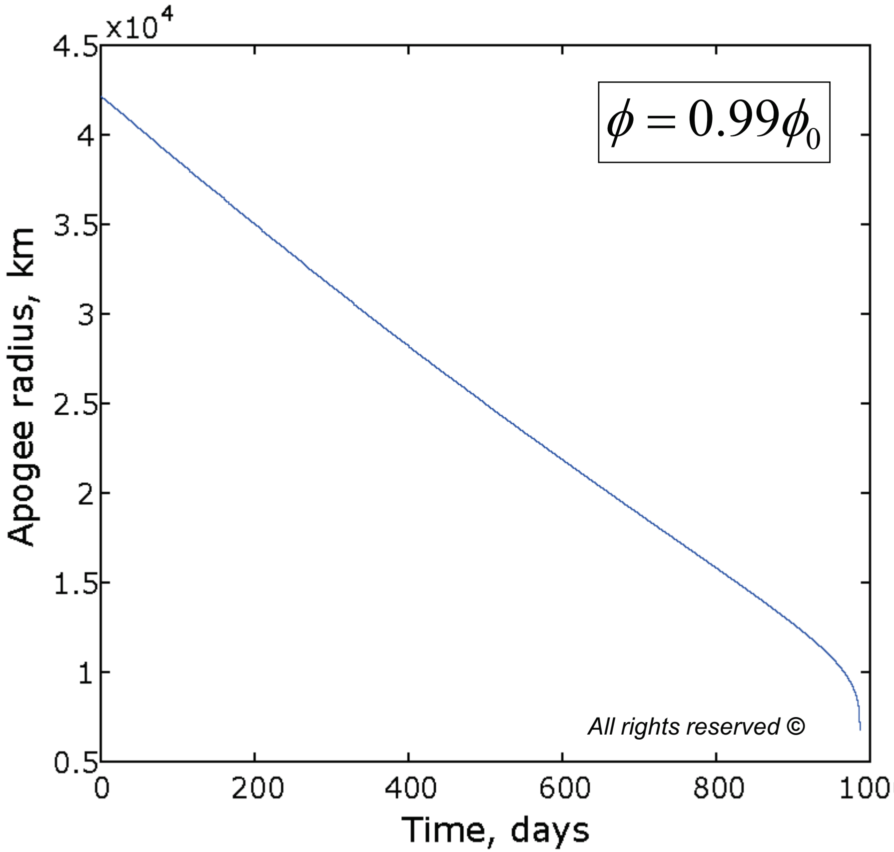

1° Analysis campaign – Single case analysis

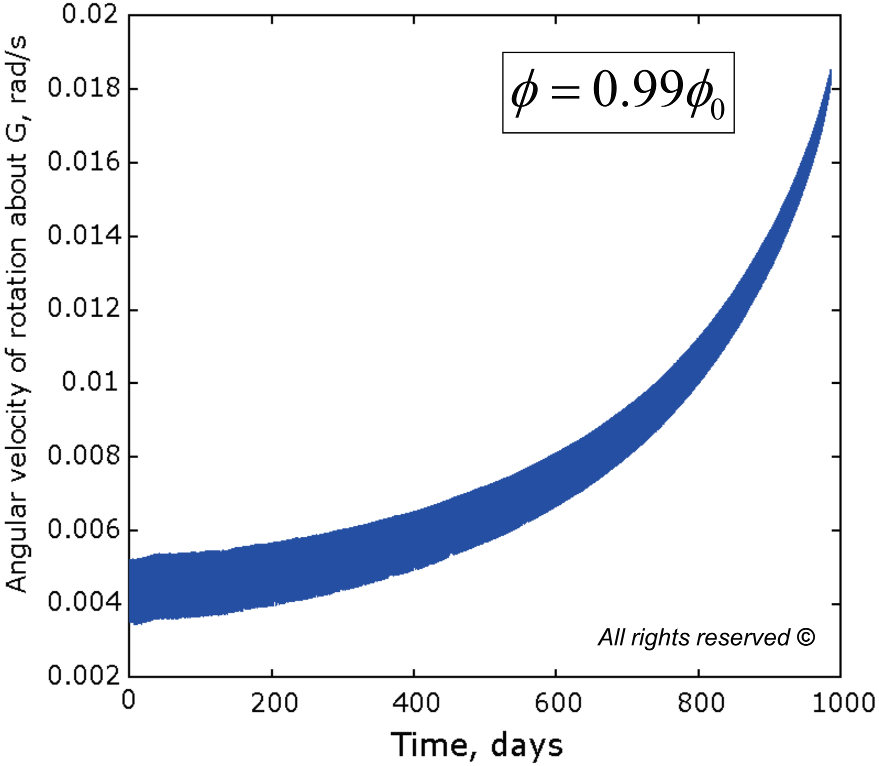

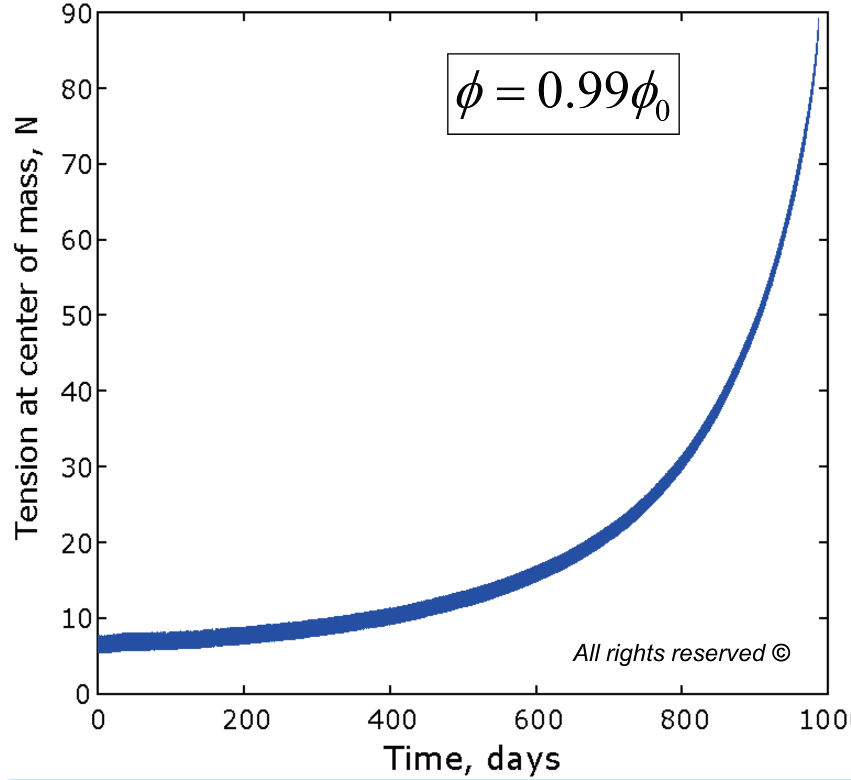

An initial angular velocity of + 0.004 rad/s is used to prevent tether slackness. The angular velocity oscillates but is always positive, i.e. local rotation in same direction as orbital motion, and constantly increasing trend.

Tension is maximum at the system's center of mass. It is mainly due to centrifugal force generated by local rotation. Oscillating behavior, always positive, constantly increasing trend. **Maximum tension of about 88 N**. Even with Al 1100 full deorbit is possible, far from breaking (and safety fac.= 3).

Deorbit time of 987 days, i.e. **2.7 years**: much lower than natural decay time that is higher than 25 years (with 90% confidence; computed with *Stela*, courtesy of *Centre National d'Études Spatiales*)

1° Analysis campaign – Multiple case analysis

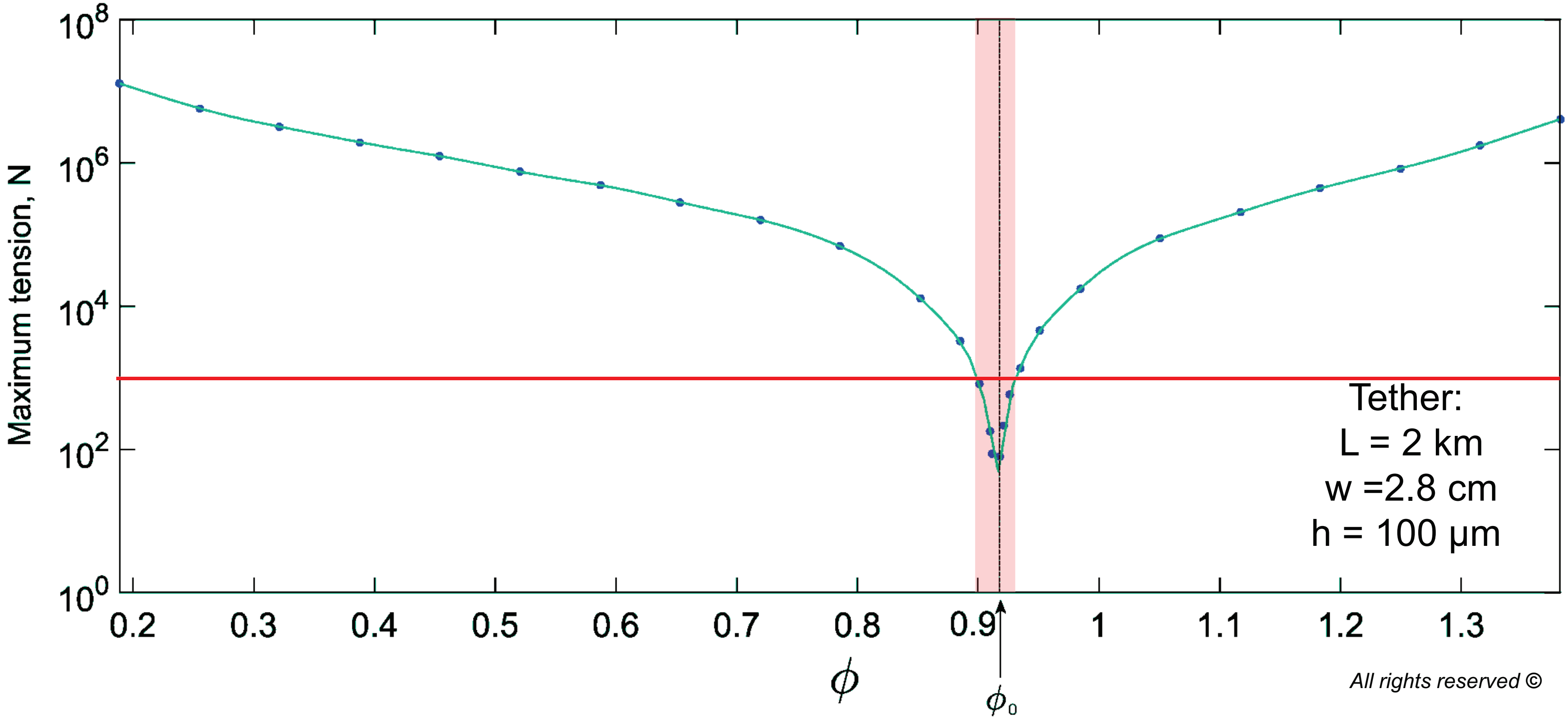

27 full deorbit simulations are run to obtain the maximum tension at center of mass during the entire deorbit, each for a different value of phi, from $\phi_{min} = \arcsin(\Lambda_t / 2)$ to $\phi_{max} = \arccos(\Lambda_t / 2)$

Knowing the tether material, the user can determine the allowed range of ϕ to avoid tether breaking. E.g. using a Metal Matrix composite with Aluminum matrix and reinforcing fibers of Nextel it is possible to reach an UTS of 1450 Mpa, and **maximum allowed tension, with safety factor K = 3, of 1750 N** leading to a **range of ϕ between 0.89 and 0.94.**

This leads to the choice of the **butterfly configuration** in the next campaign of analyses.

2° Analysis campaign – *Butterfly* configuration

One single BET subdivided in two segments of different lengths L1 and L2, and deployed on opposite directions from Sylda. Only one cathode.

- Lengths optimized to have the electrodynamic center of mass as close as possible to center of mass of the system.
- Current is generated only in the part of rotation where the electrical field is positive.

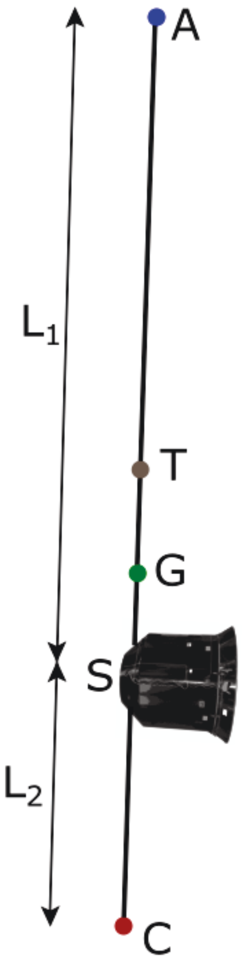

A: anode
G: center of mass of the system
C: cathode
S: object to deorbit
T: tether's center of mass

Electrodynamic drag and atmospheric drag are the dissipation forces.

Double-Dumbbell, with **Hybrid** numerical method . Nondimensional method used only for computation of average tether current.

- **Both in-plane and out-of-plane dynamics are considered, and variation of all orbital parameters.**
- Geomagnetic field with higher harmonics
- IRI-2011 database from NASA for plasma electron density, with average Solar flux activity
- Jacchia-Bowman 2008 for atmospheric density, with average Solar flux

2° Analysis campaign – Equations of the model

Refer to PhD thesis after its publication.

Equations of **global motion** of the system's center of mass along the deorbit path

Refer to PhD thesis after its publication.

Equations of local in-plane and out-of plane rotational motion of the system around its center of mass

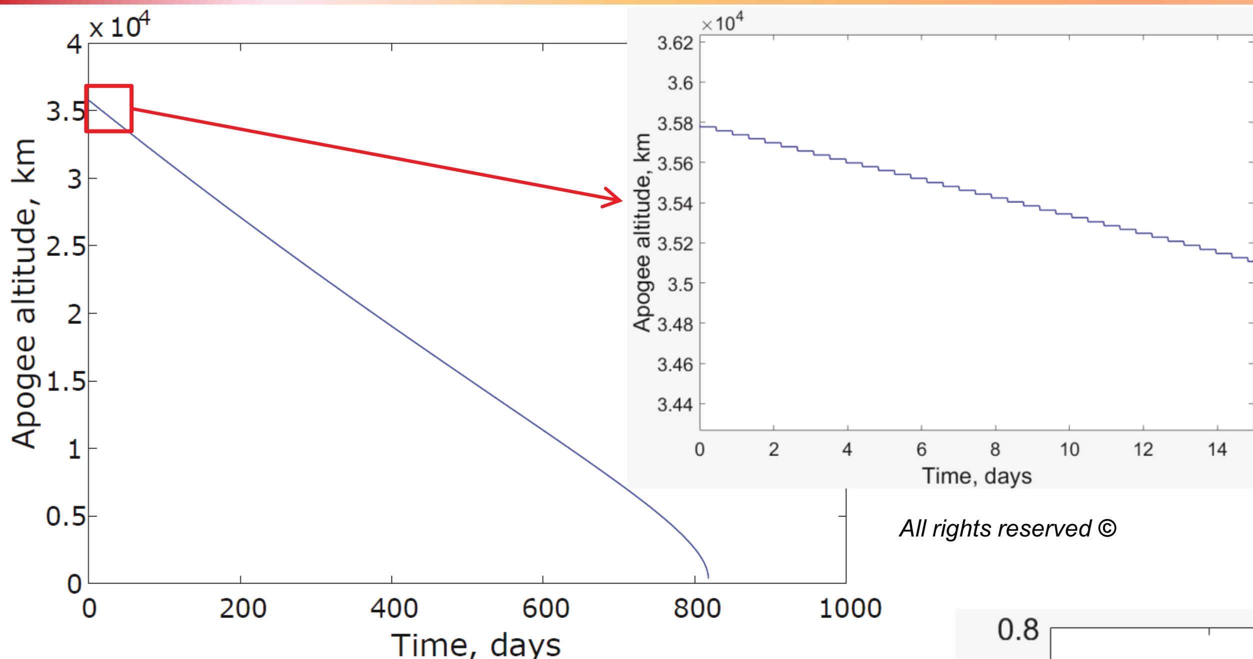

Continuosly decreasing profiles for apogee altitude, perigee altitude, and orbital eccentricity.
Step-by-step decrease since dissipation occurs only during transits below 2000 km.
Steeper decrease in the very last part of deorbit since the system is always below 2000 km.

Deorbit time of 818 days with tether of 2 km length (L1 = 1200 m, L2 = 800 m), width of 3 cm, thickness of 100 micro-m.

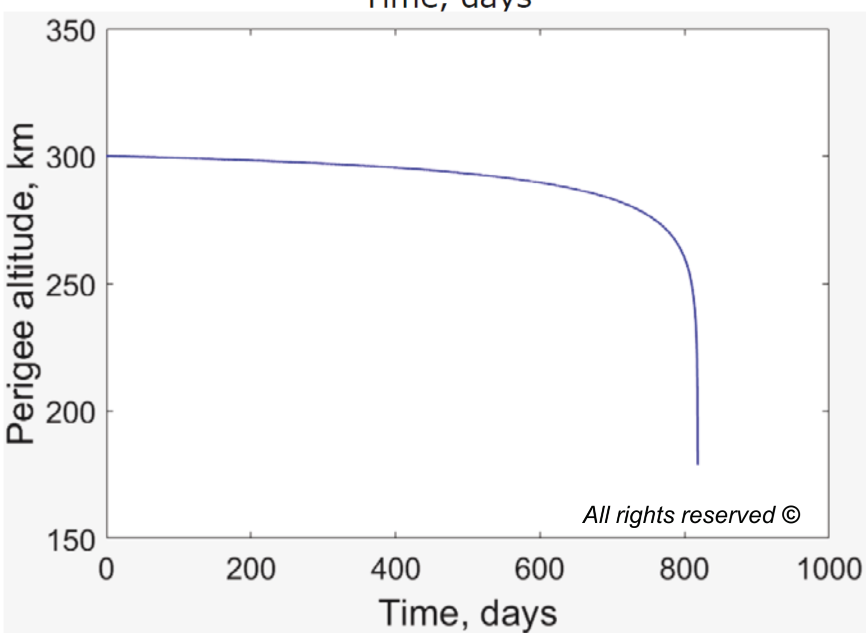

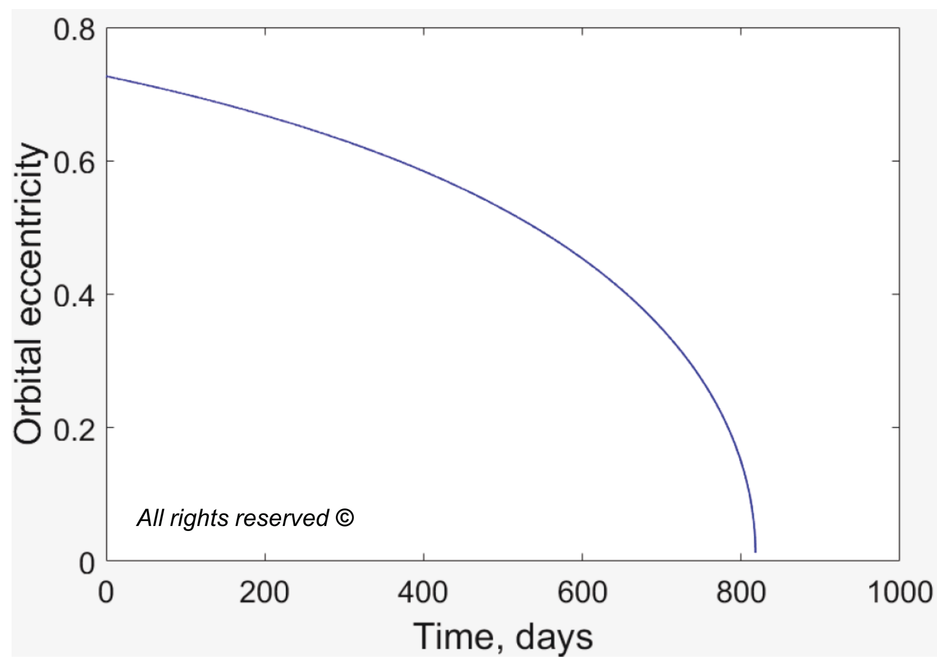

2° Analysis campaign – Results (part 2)

Small change in orbital parameters: **inclination, RAAN, argument of perigee** during deorbit.

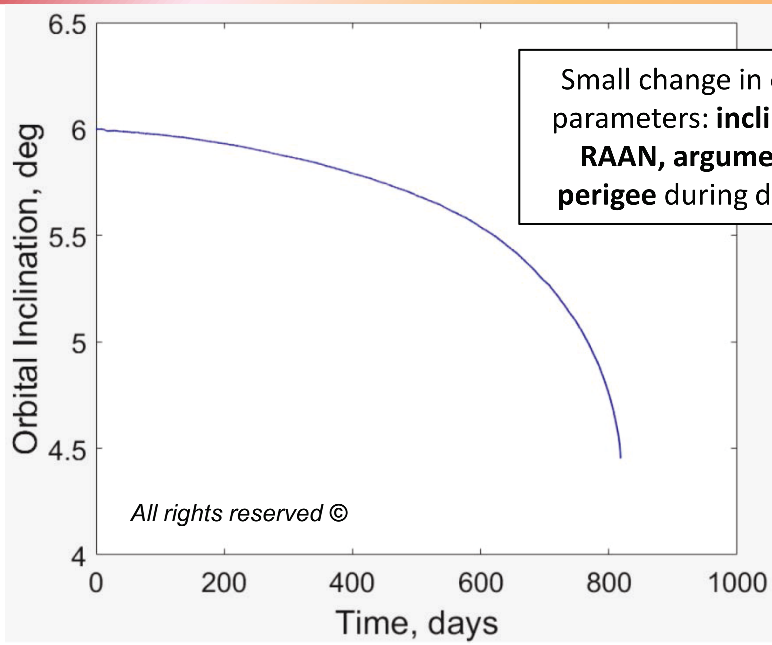

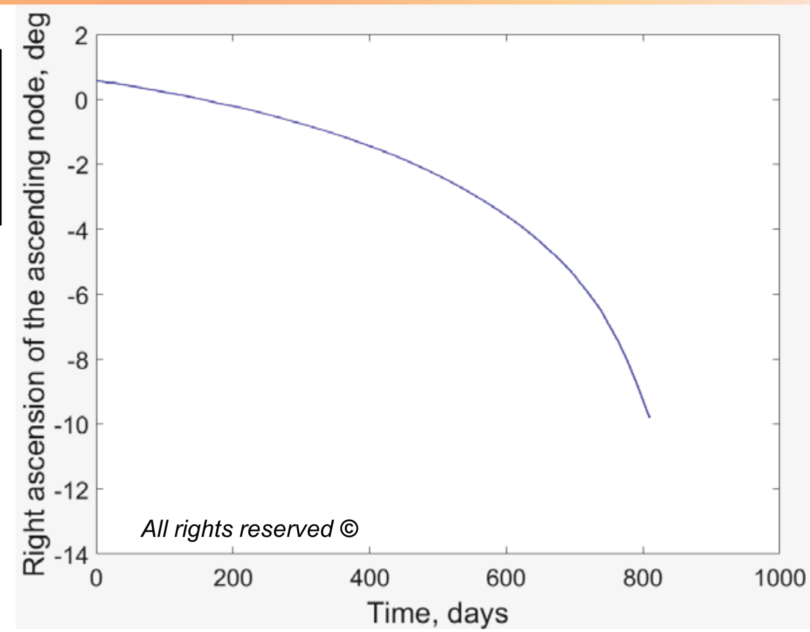

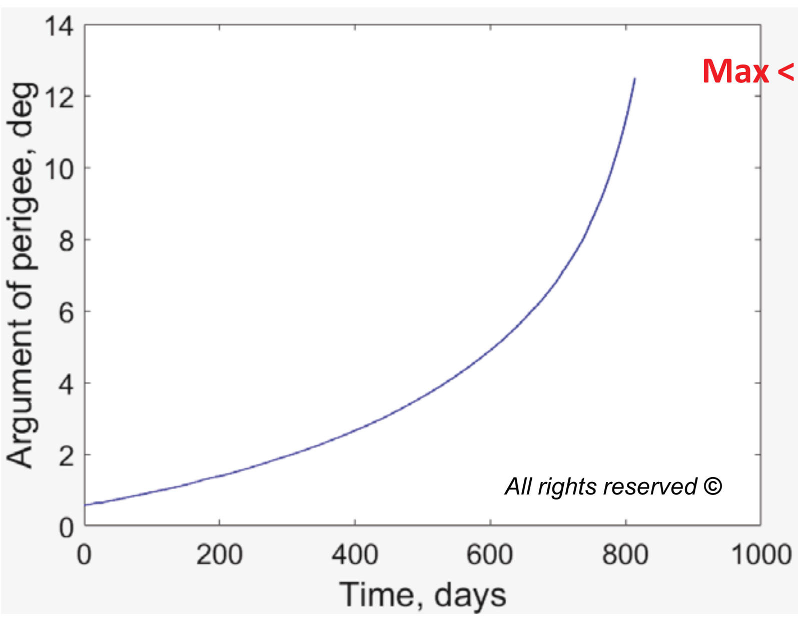

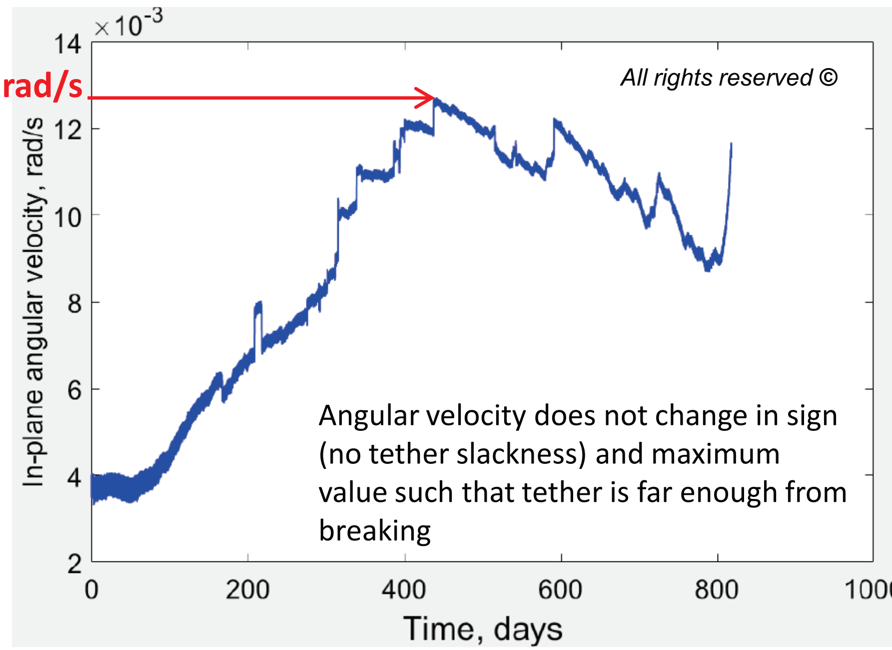

2° Analysis campaign – Results (part 3)

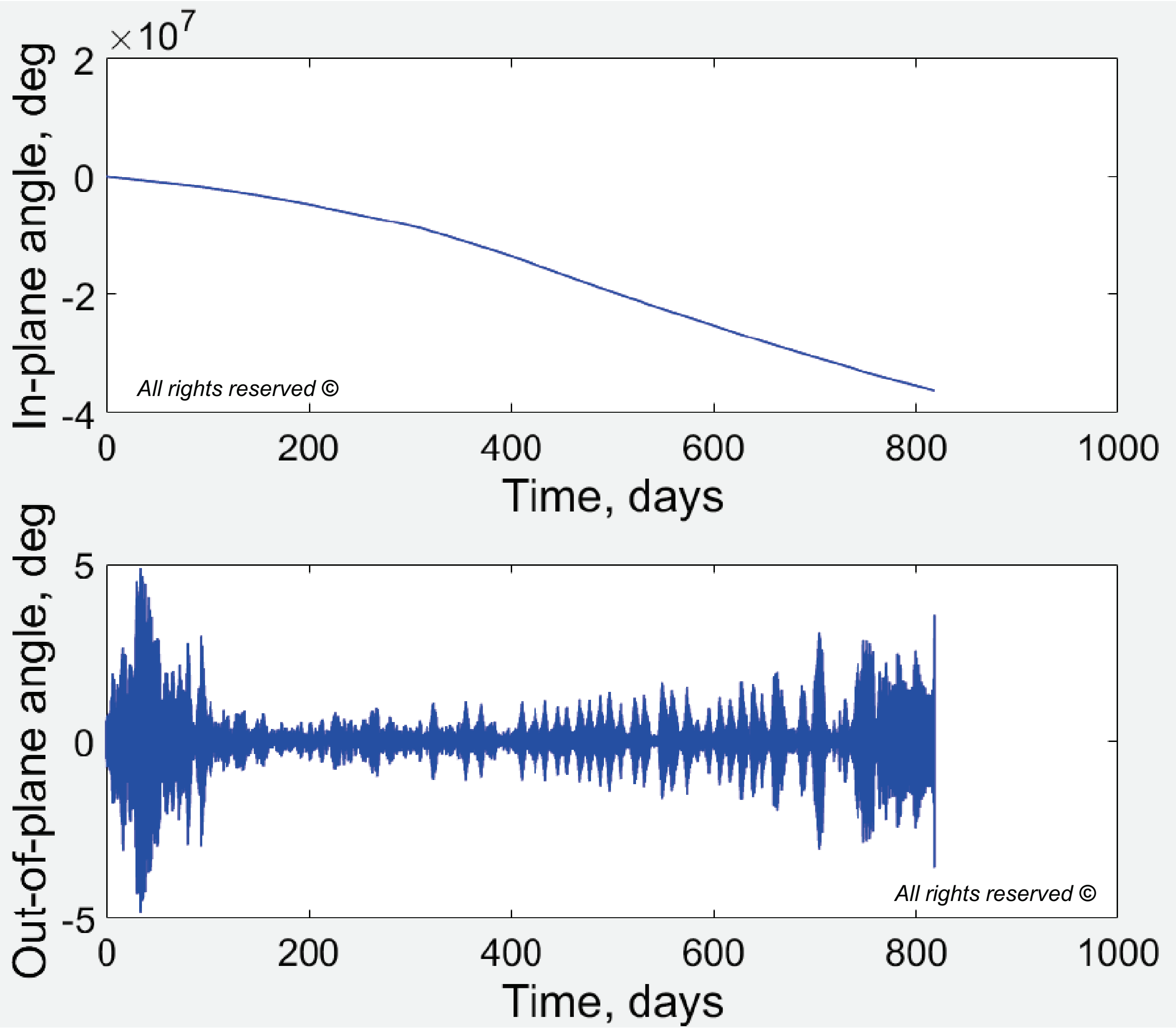

Magnitudes of:

- **In-plane angle** has an increasing trend throughout deorbit

- **Out-of-plane angle** is limited to about 5 degrees throughout deorbit, demonstrating the prevalence of in-plane motion above the out-of-plane motion.
  As reported in literature, and validating assumption of neglecting out-of-plane dynamics on 1° analysis campaign.

Part 2

ANALYSIS of PRE-DEORBIT PROCEDURES

Detumbling of Sylda

Sylda is rotating, after its release in GTO, with angular velocity of about 0.35 deg/s around the three body axes. Before deployment, it must be detumbled in order to have correct deployment without risk of interference between tethers and Sylda.

A **detumbling system based on Magnetic Torquers** is proposed:

• 2 Magnetic Torquers for detumbling about X and Y axes (e.g. Cayuga Astronautics torquers, 1.5 m long)

• 4 magnetic torquers for detumbling about Z axis: placed axial-symmetrically (e.g. Cayuga Astronautics torquers, 0.75 m long)

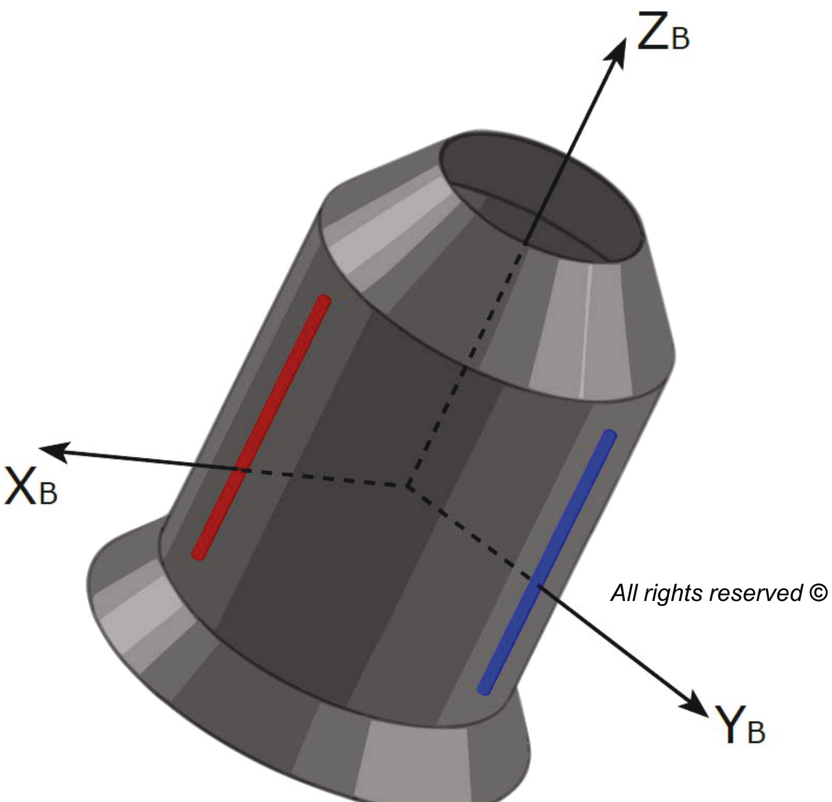

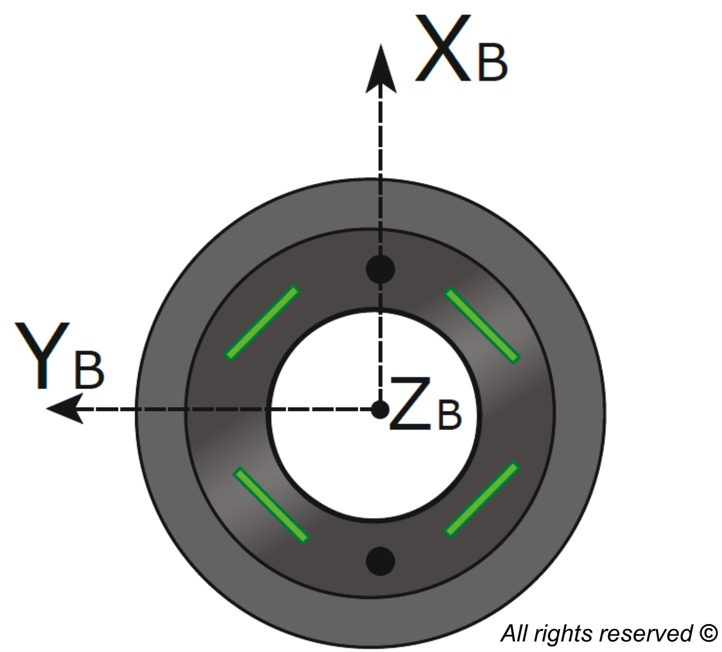

Detumbling of Sylda

Torque

Geomagnetic induction

$$M_m = m_m \times B$$

Magnetic moment along the axis of magnetic torquer: from the manufacturer's brochure

- Euler equations are used, considering the average torque created at LEO altitudes.
- Detumbling takes place during the first transit across the perigee region below 1500 km, and takes about 9 minutes around the longitudinal axis Z, and 12 minutes around the transversal axes X and Y.

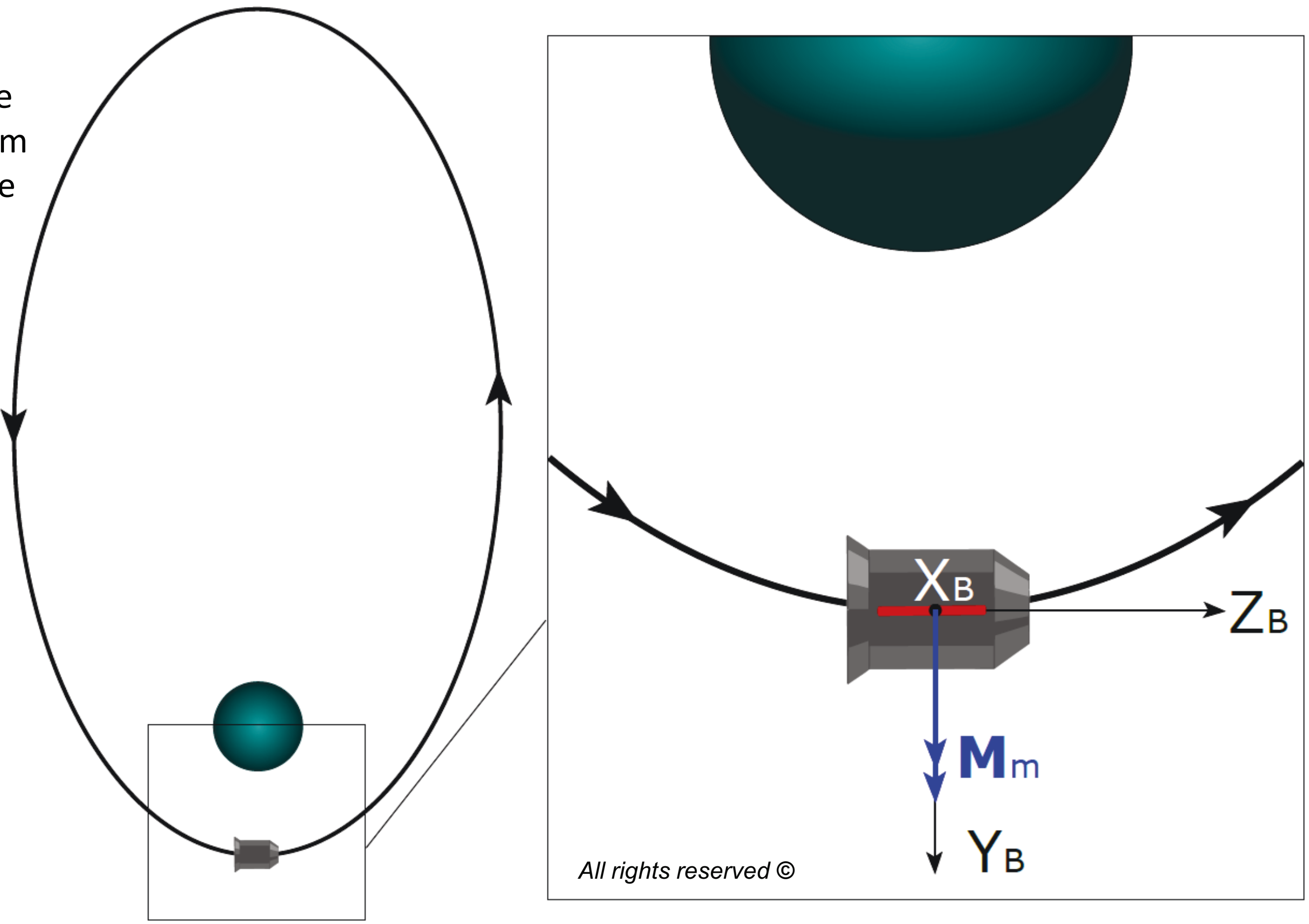

Tether storage and deployment control

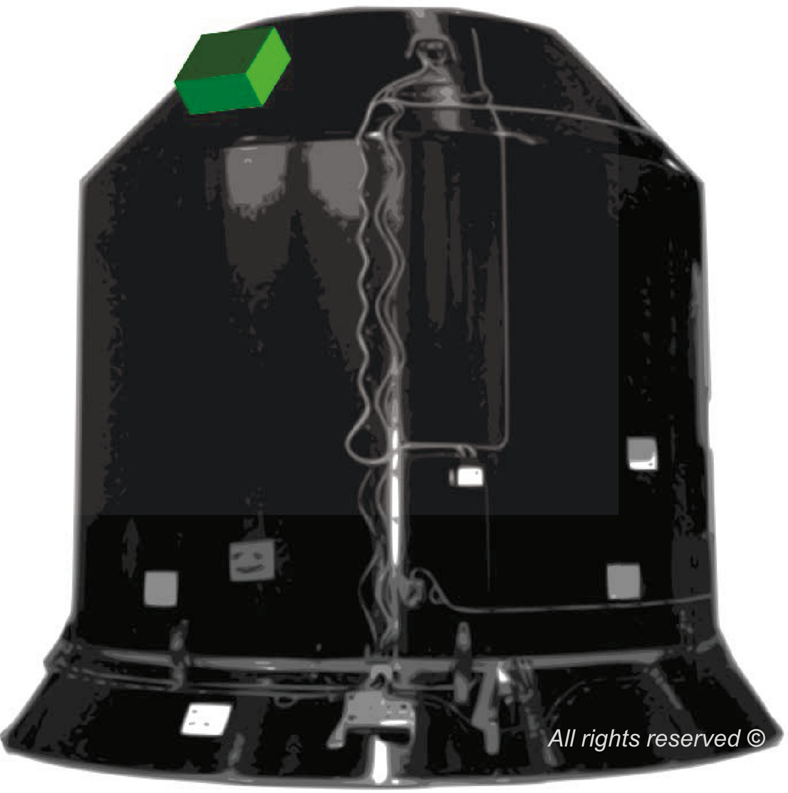

Tether reeled up around a drum wheel and stored in a dedicated box, attached to Sylda on the upper part. Two boxes, one for each tether segment, electrically connected.

- **integration to Sylda with minimum interference**: mounting where there is a large clearance from the fairing's walls, no occupation of payload envelope

- **tether stored on a spool protected inside a box**, can sustain at best vibrational loads at launch

- the deployment is eas

-**Minimize center of mass displacement**: each tether segment of the "butterfly" system stored in a dedicated box. The two boxes are mounted axial-symmetrically.

Deployment control

Deployment must be started with an initial impulse (such as a mechanical spring system) and controlled with a small electrical motor that can be powered at first with a dedicated primary battery, and then also with the electrical current passively generated along the tether. **Motor** with pre-set tether release velocity profile, **enhanced by feedback from attitude detection vision system**.

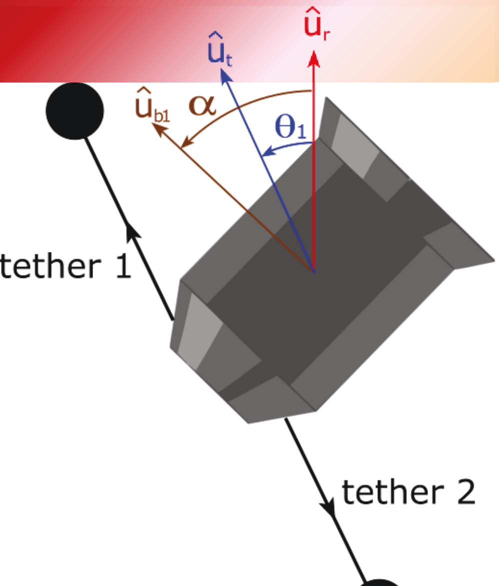

❖ ***2 Bare Electrodynamic Tethers*** (BETs) in butterfly configuration. The tape-BET tethers have lengths of 1200 m and 800 m, made of Fiber-Reinforced Aluminum, width 3 cm, and thickness of 100 micro-m.

❖ A ***hollow cathode***, on one of the two tip-masses, for electron emission

❖ A ***tipmass of 5 kg*** at each tether end.

Numerical model to simulate the deployment on the orbital plane:

- The two tethers rotate, about their attachment point on Sylda, of angles θ_1 and θ_2 on the orbital plane. The tethers rotation is separated from the local rotation of Sylda, defined by the angle **α**, and affected by tension exerted by tethers. Both angles are measured with respect to the orbital frame.

- The tethers are deployed with an initial angle of 30-45 degrees with respect to the local radial vector.

- Three cases of deployment are analyzed:

1) **Deployment at apogee**
2) **Deployment at perigee**
3) **Deployment at mid-way along the GTO, above 2000 km**

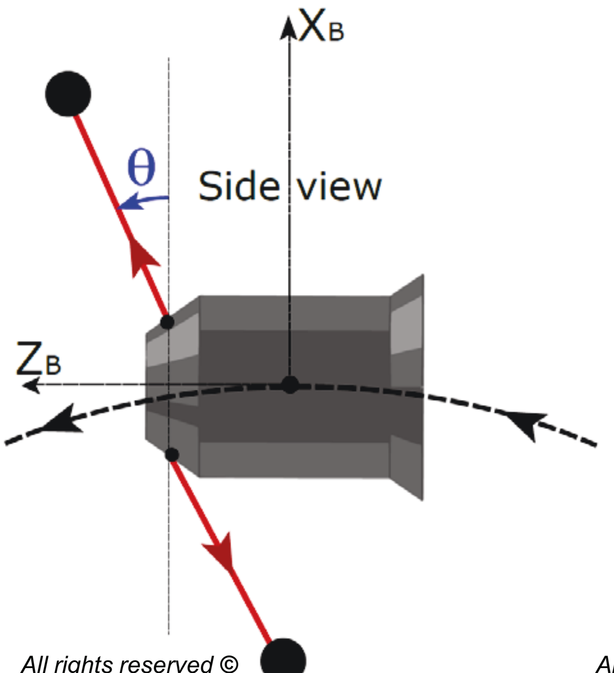

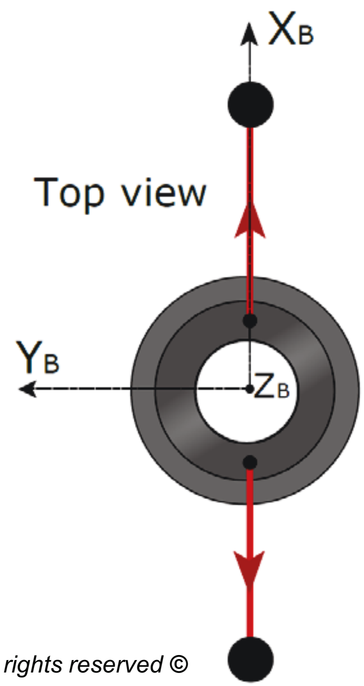

Deployment at perigee

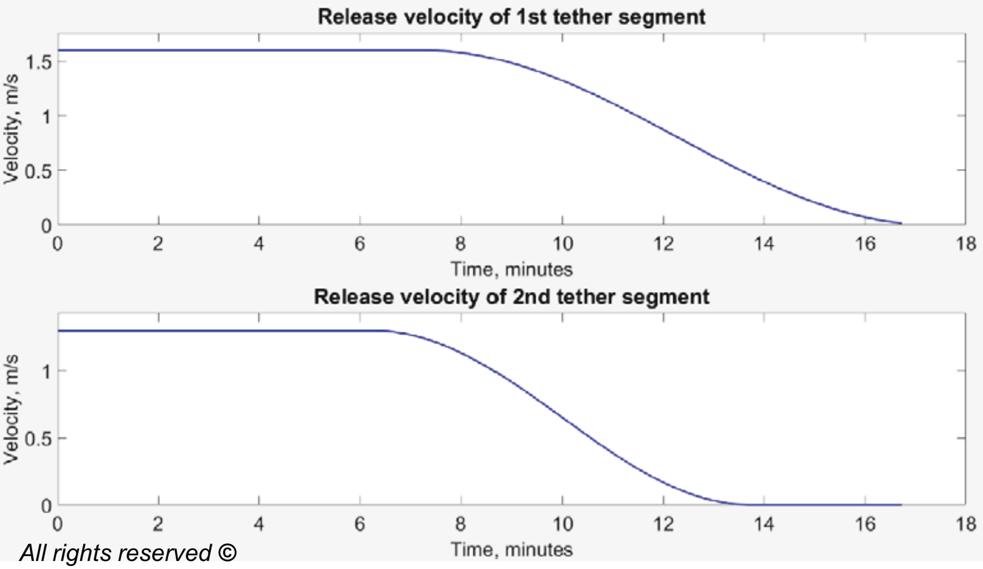

• **Two tether segments are considered, rotating with independent angles θ_1 and θ_2 .** Dumbbell model, tip-masses of 5 kg. Sylda rotates with angle **α**, that is independent from the tethers rotaion, but related due to moments exerted by tether tension at attachment points.

• The two tether segments are deployed with **constant but different release velocities until a prescribed time, and then the deployment velocity decreases** with zero tangent and **zero release velocity** in order to prevent a mechanical shock. Deployment of one segment can finish at a different time than the other.

Perturbations are considered: electrodynamic and atmospheric drag. Tip-mass, due to perturbations, shows a non-regular path during deployment: possible interference between the tether segments and Sylda's body (risk of wrapping of the tether around Sylda). **Deploying at perigee should then be discarded**.

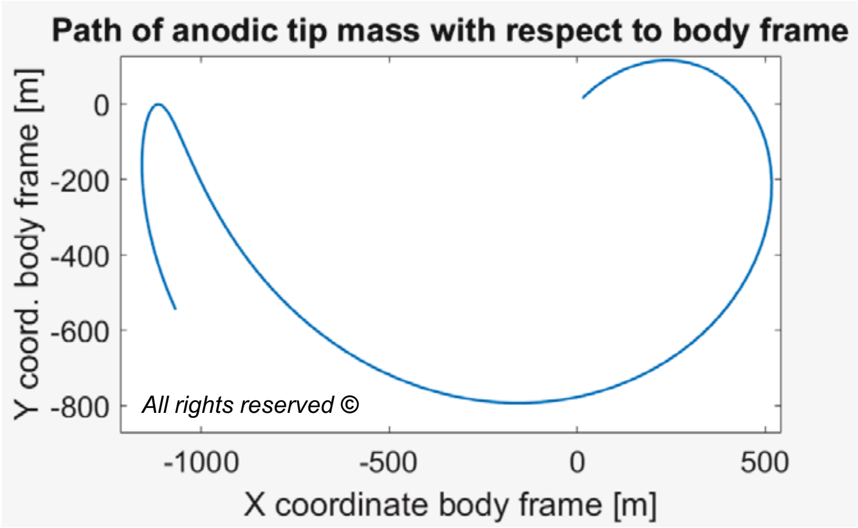

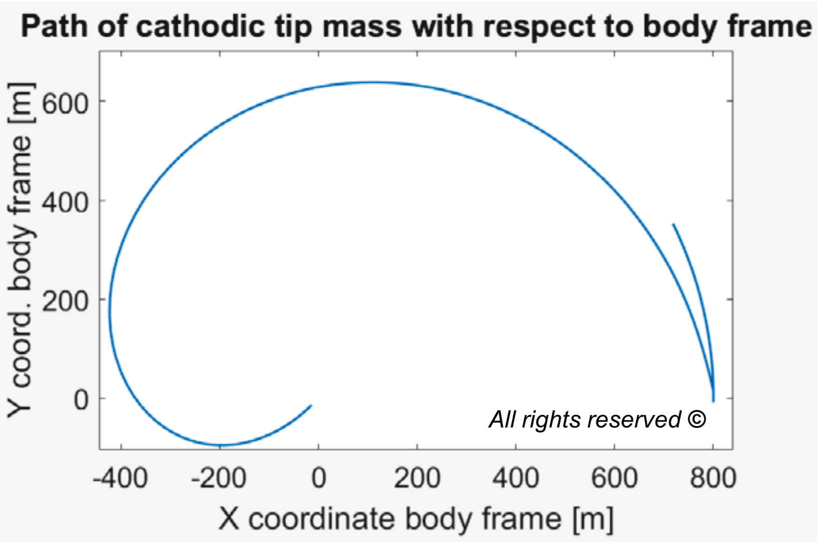

Deployment at mid-way

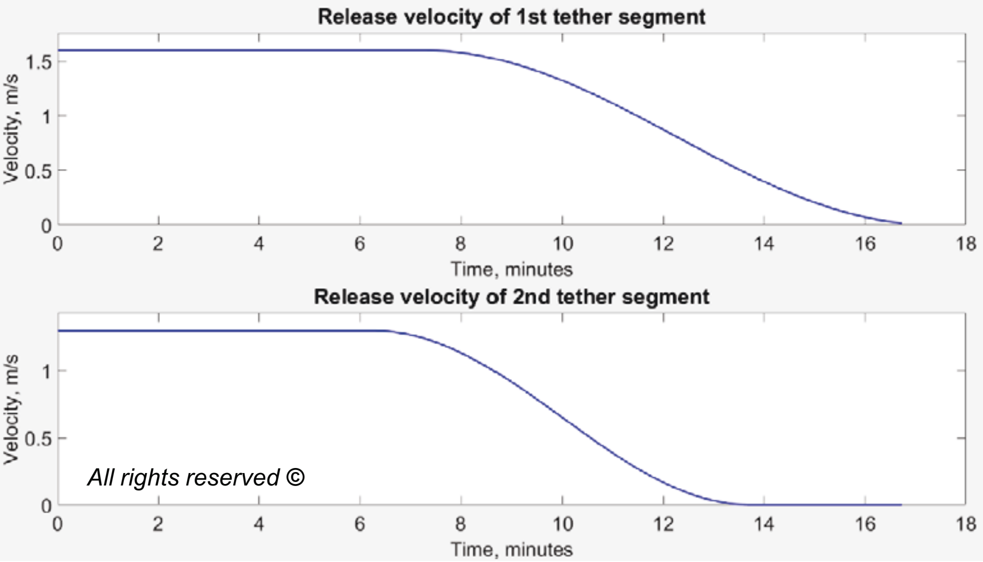

- **Two tether segments are considered, rotating with independent angles θ1 and θ2 .** Dumbbell model, tip-masses of 5 kg. Sylda rotates with angle **α**, that is independent from the tethers rotaion, but related due to moments exerted by tether tension at attachment points.

- The two tether segments are deployed with **constant but different release velocities until a prescribed time, and then the deployment velocity decreases** with zero tangent and **zero release velocity** in order to prevent a mechanical shock. Deployment of one segment can finish at a different time than the other.

No perturbations are considered: deployment takes place above 2000 km while Sylda leaves the perigee region towards apogee. This is the optimal choice for deployment for two reasons: **1) start right after detumbling across the perigee region**; **2) the tip-masses, one at the end of each tether, show a regular path with respect to body axis X**. No risk of interference between tether segments and Sylda; tethers and Sylda start to rotate together at the end of deployment.

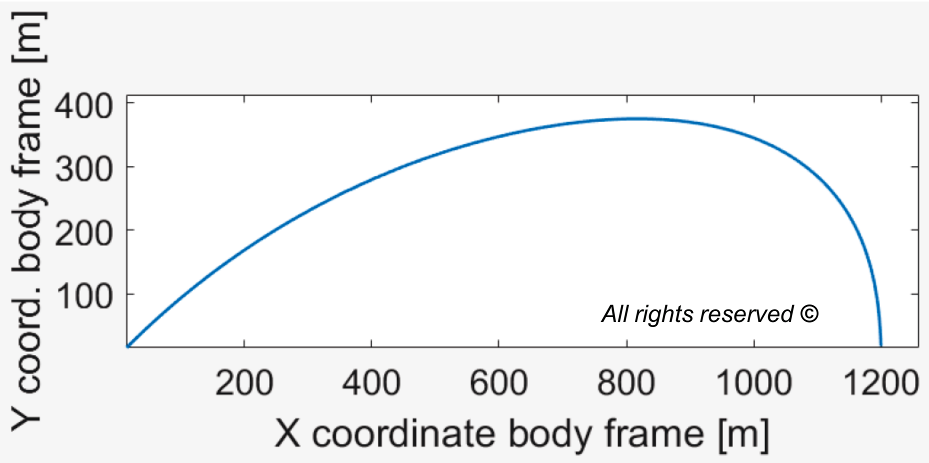

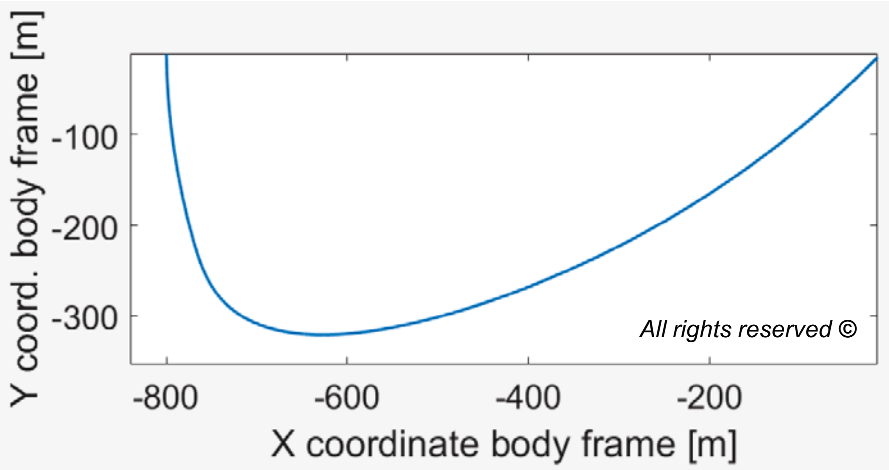

Part 3

ANALYSIS of VISION SYSTEM

Measurement system to track the motion of each each tip-mass during deployment: **1 or 2 cameras**.

From previous deployment analysis, it is computed the profile of angular position (θ) of the tip-mass on the orbital plane, with respect to the optical axis, VS tip-mass spatial coordinate (Z =X body).

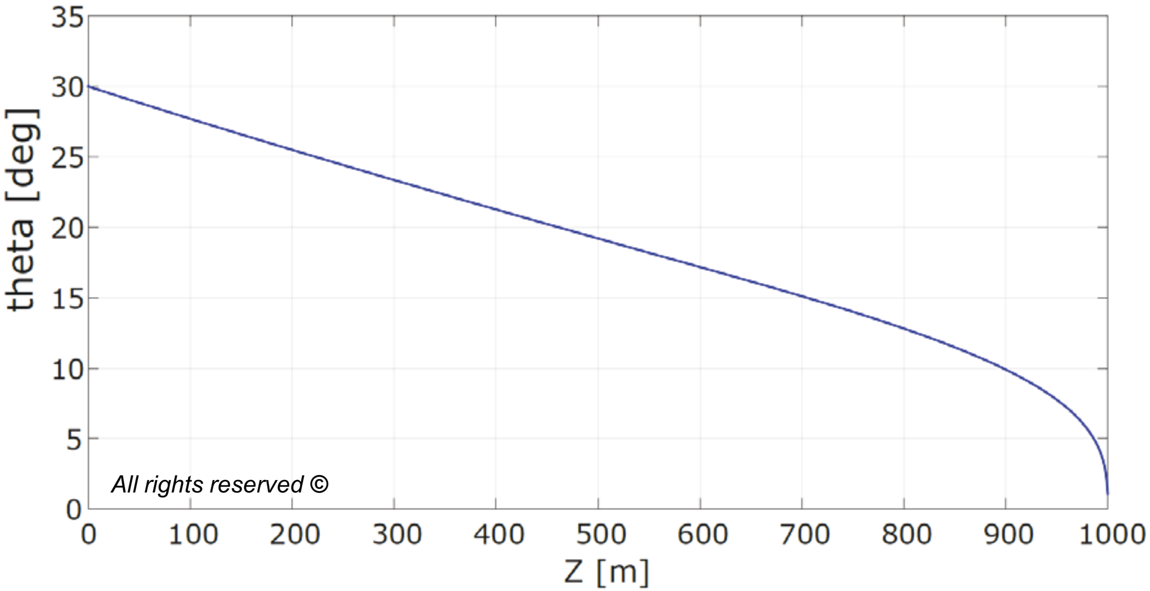

OBJECTIVE

Evaluate the accuracy of different configurations of vision system in detecting the angle θ and the distance Z during deployment, starting from a minimum detectable distance Z_{min}.

The uncertainty affecting the measure is then evaluated.

Two possible scenarios

1) Only the angular position of the tip-mass (angle θ) is measured.
2) Both angular position θ and distance Z of the tip-mass are measured.

Two cameras for each tip-mass, with different FOVs and focal lengths

1st camera optimized to detect the tip-mass in the first part of deployment (from Zmin to Z')

2nd camera optimized for the second part of deployment (from Z' to Zmin).

Zero baseline between the cameras: not a stereo system but a combination of two monocular systems.

Focal length

$$f = \frac{L}{2\tan\left(\frac{FOV}{2}\right)}$$

Angular resolution

$$\Delta\theta \approx \frac{FOV}{N_P}$$

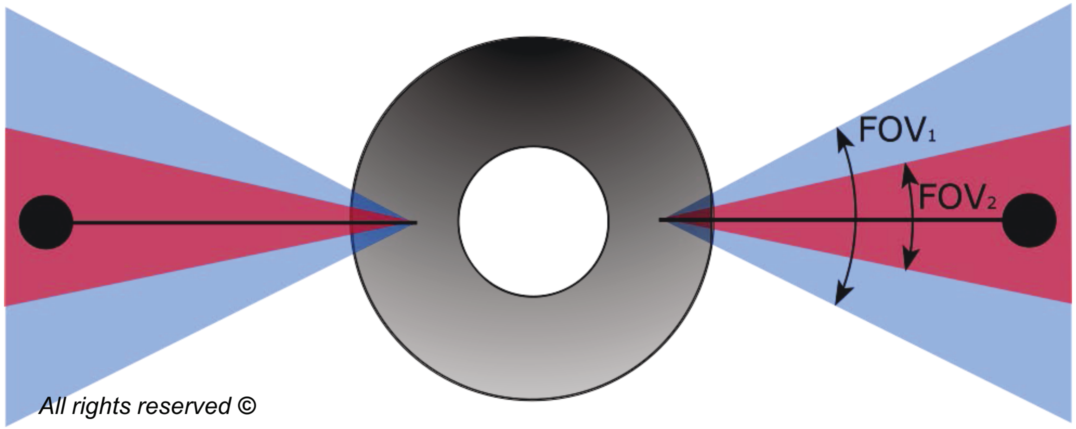

Standard uncertainty due to angular resolution Δθ, with uniform Probability Density Function

$$\sigma = \frac{\Delta\theta}{2\sqrt{3}}$$

The two cameras have the same sensor size L and number of pixels Np

Camera 1 needs a larger FOV in order to detect at best the first part of deployment, where the angle θ is larger. FOV_1 defined by the angle θ at the minimum detected distance Z_{min}, i.e. at the beginning of deployment, starting with a non-zero in-plane angle with respect to the optical axis.

$$FOV_1 = 2\theta_{Z,\min}$$

The tether tends to align to the optical axis towards the end of deployment, therefore the angle θ becomes lower and lower. Thus, FOV_2 of camera 2 must be lower, so the angular resolution (and then higher accuracy).

$$FOV_2 = 2\theta_{Z'}$$

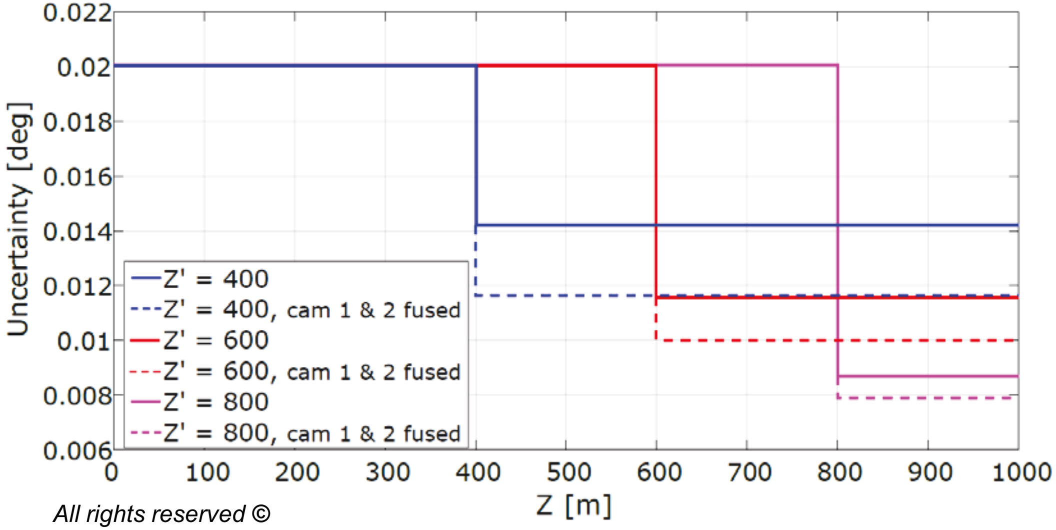

Z’ is the tip-mass distance until which only camera 1 is detecting the tip-mass angular position. The FOV of camera 2 depends on Z’: increasing Z’ means lower FOV and lower uncertainty for camera 2, but at the same time a higher uncertainty for longer time of use of only camera 1.

By using a Kalman filter to fuse the detection of camera 1 and 2, for Z > Z’, there is a reduction of uncertainty (dashed lines). Continuous lines means using only camera 2 detection for Z > Z’.

RED line: only camera 1 used for Zmin < Z < Z2,min, and then only camera 2 for Z’ < Z < Zmax.

BLACK line: only camera 1 used for Zmin < Z < Z2,min, and then fused 1&2 with Kalman filter for Z’ < Z < Zmax.

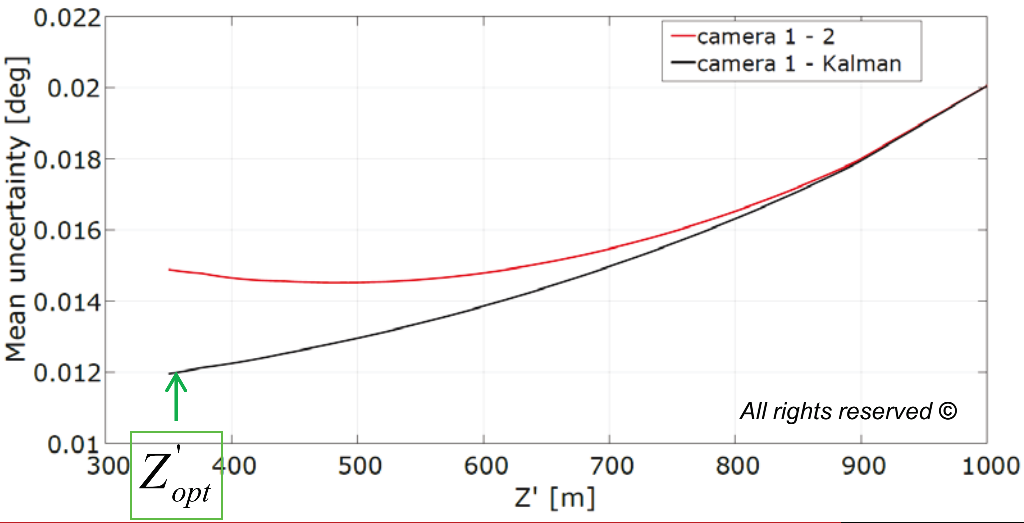

The aim is to find the optimal Z’ to choose in order to have the minimum mean uncertainty on the measure of θ during deployment.

Optimal condition

Z’opt = Z2,min = 350 m

+

fused 1 & 2 cameras with Kalman filter for Z’ < Z < Zmax

2nd scenario: tip-mass direction and distance

All considerations regarding uncertainty in detection of direction θ are identical to first scenario.

Analyzed the **uncertainty** in detection of **distance Z** considering two options:

1) Monocular system

One camera for each tip-mass.
Mounted on the upper conical part of Sylda.

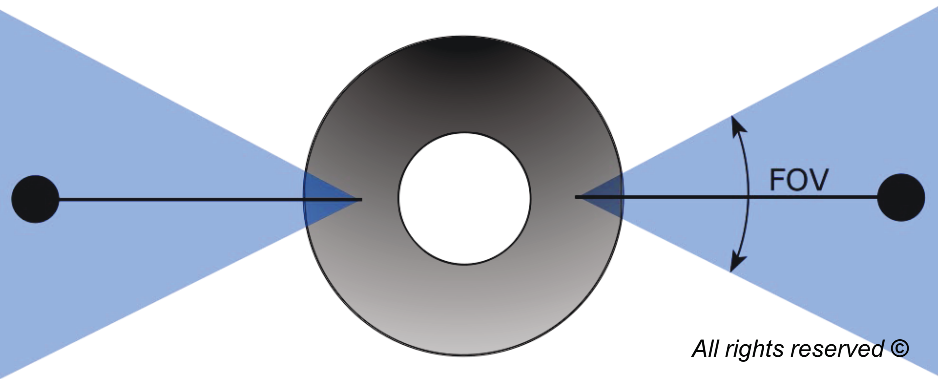

Target to detect (i.e. tip-mass) is equipped with a planar pattern. 4 features always detectable by the camera: 3 on a circumference of radius 0.5 m to form an equilateral triangle; 1 at the orthocenter.

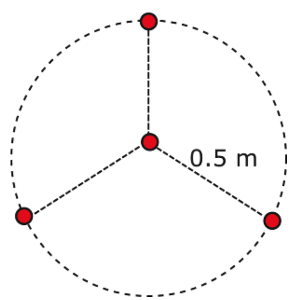

The distance is estimated from detecting the pose of the tip-mass, using the P3P solver proposed by Kneip et al. The uncertainty on the distance takes into account only the contribution of the sensor resolution (σr) .

2) Stereo system

Baseline between the two cameras is b = 4 m, mounted on the upper conical part of Sylda. Tip-mass modeled as a point mass, and assumed to be always detectable by the stereo system. The optical axes of the two cameras are aligned and their FOVs are identical.

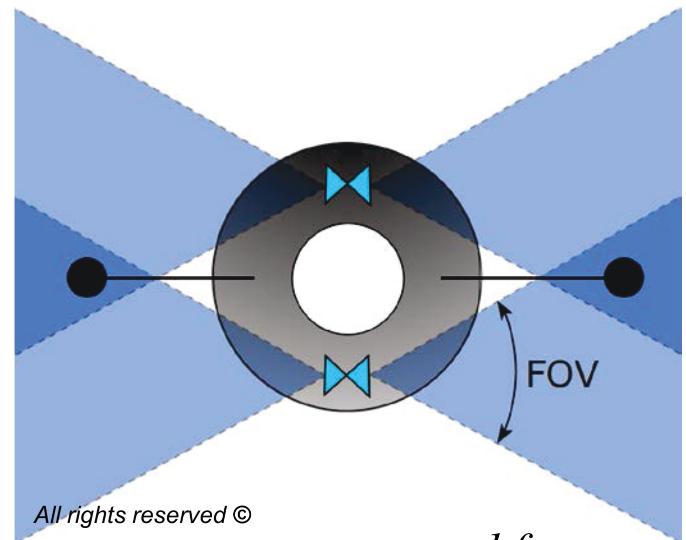

The distance is estimated as: $Z = \frac{bf}{d}$

Where f is the focal length of and d is the disparity (i.e. distance in image coordinates between the projection of the tip-mass in left and right camera).

2nd scenario: tip-mass direction and distance

In case of **monocular system**: the maximum uncertainty in distance Z is variable with tip-mass orientation. E.g. for roll angle Φ=0, the higher is the pitch angle Θ (rotation about normal to orbital plane) the lower is the uncertainty.

The uncertainty in the measure of distance Z, using a **stereo system**, is **always lower with respect to the uncertainty with the monocular system** (where only σ_r was considered). **<u>The stereo system is then the optimal configuration.</u>**

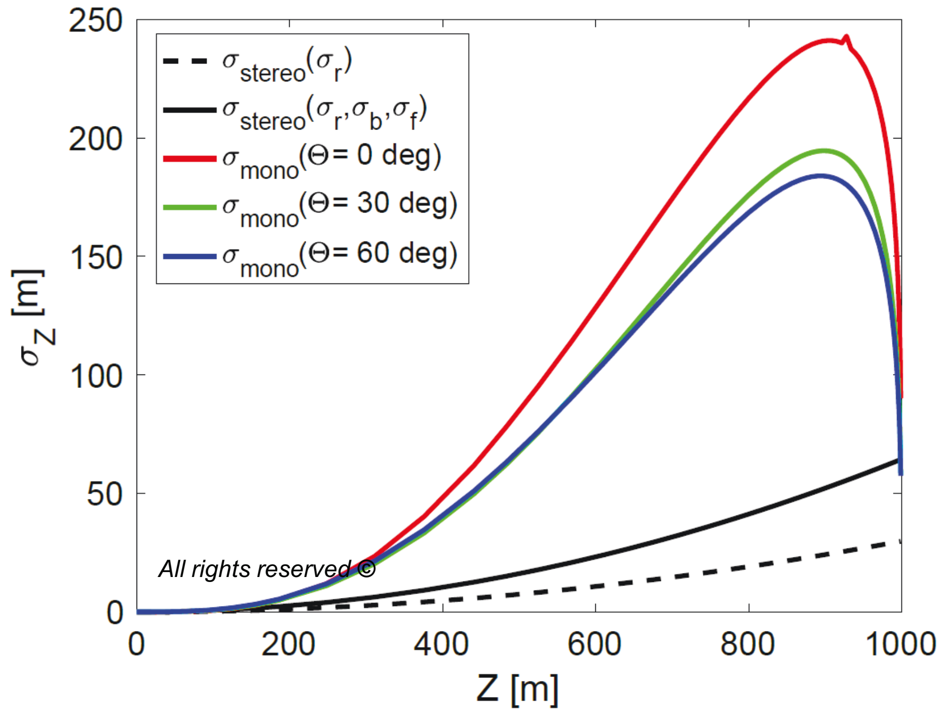

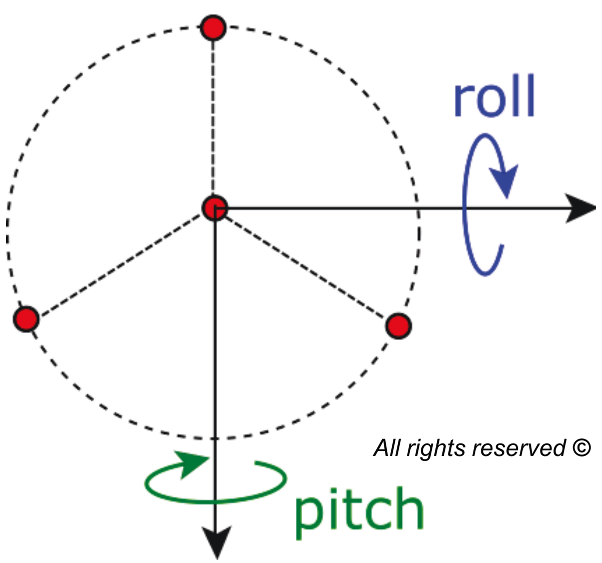

The uncertainty increases with increasing roll angle Φ.

TABLE II
PEAK VALUES OF THE UNCERTAINTY ON THE MEASURED POSITION CONSIDERING DIFFERENT ORIENTATIONS OF THE TIP MASS WITH RESPECT TO THE CAMERA FIXED REFERENCE FRAME.

$\sigma_{\max}(\Phi,\Theta)$ [m]	$\Theta = 0$ deg	$\Theta = 30$ deg	$\Theta = 60$ deg
$\Phi = 0$ deg	242.96	194.57	183.95
$\Phi = 15$ deg	248.09	230.51	213.97
$\Phi = 30$ deg	247.83	250.00	238.40
$\Phi = 45$ deg	256.39	265.25	259.58

CONCLUSION

Conclusive remarks

Deorbit of Sylda from GTO (after full tether deployment):

1. Deorbit without tether instability requires to start with a minimum angular velocity of the BET system of local rotation around its center of mass
2. Deorbit without tether breaking requires a butterfly configuration, in order to have the system's center of mass as close as possible to the electrodynamic center of pressure during deorbit. Tether resistance is increased using Fiber-Reinforced Aluminum instead of pure Aluminum.
3. Deorbit without instability and tether breaking can take place successfully, under the reasonable assumptions considered in the model, in a time of about 2.2.-2.7 years (depending on the model considered) << than the 25 years set by guidelines for debris removal.

Pre-deorbit procedures:

1. Detumbling of Sylda is necessary around the three body axes: it can be performed during the first passage across the perigee region, in about 9-12 minutes, with a set of *magnetic torquers*.
2. The two tether segments of the butterfly system can be stored around spools in separate boxes placed axial-symmetrically on the upper part of Sylda. A small electrical motor is used to control the tether release velocity, enhanced by the feedback provided by a vision system for attitude detection.
3. Deployment of the tethers must be performed after detumbling, and after Sylda surpassed about 2000 km of altitude while going back towards apogee, i.e. at mid-way of its first orbit.

Vision system for attitude detection:

1. When detecting the angular position of the tip-mass, the best performing configuration is: 2 monocular cameras and their measure fused by Kalman filter after a certain deployed length of tether.
2. When measuring the distance of the tip-mass, the best performing configuration is in any case a stereo system for each tip-mass, with baseline of 4 m between the two cameras of each couple.

Publications and conferences

M.Pertile, M. Mazzucato, G. Pastore, A. Valmorbida, S. Chiodini, R. Giubilato, S. Debei, E.C. Lorenzini, *"Comparison of Vision System Approaches for Distance Measurement of a Tether Tip-Mass during Deployment on High Eccentricity Orbit."* - 25° Congresso Nazionale di Misure Meccaniche e Termiche (GMMT), part of 1° Forum Nazionale delle Misure. Modena. September 13-16, 2017.

M. Mazzucato, G. Pastore, M. Pertile, E. Lorenzini, *" Vision System for Tether Tip-Mass Detection during Deployment on High-Eccentricity Orbit"* - 2017 IEEE International Workshop on Metrology for AeroSpace. Padova. June 21-23, 2017.

G. Pastore, E. Lorenzini, G.Sanchez-Arriaga, *"Deorbit with Bare Tether System from High Eccentricity Initial Orbit: Analyses and Numerical Simulations".* 5th International Conference on Tethers in Space. Ann Arbor, Michigan (USA). May 24-26, 2016.